

Investigations of discrepancies between laboratory studies of the flow of ice: density, sample shape and size, and grain-size

T. H. JACKA

*Antarctic CRC, Box 252C, Hobart 7001, Australia
and Australian Antarctic Division*

ABSTRACT. Laboratory results are presented concerning ice creep at minimum creep rate (at $\sim 1\%$ strain) for fine-grained, initially isotropic, polycrystalline samples. The effect on the creep rate of ice density, sample shape (aspect ratio) and size, grain-size and ratio of grain-size to sample size is examined. Provided sample density is above $\sim 0.83 \text{ Mg m}^{-3}$ (i.e. the close-off density), there is no effect of density on ice-creep rate. Results provide no evidence of a creep rate dependence on test sample length for cylindrical samples. Sample diameter, however, does affect creep rate. Over the range of sample diameters studied (16.2 to 90 mm) creep rate decreases monotonically by a factor of ~ 4 . This effect is independent of sample aspect ratio. Experiments examining size effects in simple shear indicate no dependence of minimum flow rate on shape or size in this stress configuration. Two grain-sizes were represented within the samples tested for the effect of sample size. As expected from earlier work, no grain-size effect on minimum creep rate is evident. In addition, there was no evidence of an effect on creep rate of the ratio of grain-size to sample size.

INTRODUCTION

In a review paper examining theoretical predictions, laboratory data and field data concerned with the flow of polycrystalline ice, Hooke (1981) concluded that "The substantial discrepancies among different laboratory studies require detailed investigation. Inter-laboratory exchange of samples would facilitate resolution of this problem." Hooke considered (and rejected) three factors—density, grain-size and sample size—to account for variability he had noted among different laboratory studies. Inter-laboratory exchange of ice test samples is now occurring as part of an international collaboration (Australia, France, Denmark, Canada) concerning the flow properties of Antarctic, Agassiz and Greenland ice. In the meantime, however, laboratory studies now indicate that we may be able to account for some of the discrepancies in terms of test sample geometry.

In this paper all three of the above factors are re-examined through a series of systematic laboratory tests which compare the flow of different ice samples at minimum strain rate. Ice flow at minimum strain rate is not steady state. Minimum strain rate, however, does provide a unique, identifiable point on the ice-creep curve of particular value for comparison of the effect on the flow of parameters such as density, sample size, crystal size, etc.

DENSITY

Despite suggestions (e.g. Hooke, 1981) that density might influence the results of laboratory studies of ice flow, and that it might be one parameter which could account for discrepancies amongst the various ice deformation studies, to this author's knowledge no systematic study has been published of the effect of this parameter. Mellor and Smith (1966) carried out uniaxial compression tests on laboratory-prepared snow with densities of 0.436, 0.531, 0.644 and 0.832 Mg m^{-3} . They found that secondary strain rate increased by several orders of magnitude as density decreased over this range. Haefeli and von Sury (1975) performed compression tests on firn from Greenland at -10°C . Their flow parameter, which represented a shear velocity under a unit shear stress, increased by approximately two orders of magnitude as density decreased from 0.75 to 0.47 Mg m^{-3} .

Here, the effect of density on minimum ice-creep rate is studied, particularly in the range of densities above and below 0.83 Mg m^{-3} , this being near to the value at which close-off (interconnecting air passages between firn grains are sealed off) occurs in natural ice masses (Paterson, 1981).

Twenty-three cylindrical ice samples were tested. Four of these were of isotropic ice, prepared by the method described by Jacka and Lile (1984). The density of each of these samples was 0.912 Mg m^{-3} . The remaining 19

samples were cut from different depths of an ice core (BHQ, Law Dome, Antarctica) exhibiting different densities. Samples were cut such that the compression axis was near to parallel to the core length. Each sample was machined to 25.6 mm diameter, while lengths ranged from 39.3 to 58.7 mm.

Thin sections were cut from each sample before and after testing, with normals parallel to the compression axis. C-axis orientations were measured under a modified Rigsby stage (Morgan and others, 1984) and were plotted on Schmidt equal-area nets. Each orientation fabric exhibited a near-random pattern prior to testing.

A direct-load uniaxial compression apparatus (Jacka and Lile, 1984) was used to deform samples to beyond minimum strain rate. Strain was estimated from the linear shortening (measured with dial indicators resolvable to 0.001 mm) of the ice sample in these constant load tests. Tests were carried out at an octahedral shear stress of 0.2 MPa and at a temperature of -3.3°C. Temperature was maintained by enclosing the entire compression apparatus in an insulated box in which the air temperature was thermostatically controlled using a method based on the technique described by Morgan (1979). Usually for deformation tests, to avoid ablation of the ice sample it is immersed in a fluid bath of silicon oil or kerosene. However, for the current set of tests, since

many of the samples were porous, they were not immersed in a fluid, but completely covered with petroleum jelly.

Table 1 presents the results of the 23 tests. Figure 1 is a plot of minimum octahedral shear strain rate as a function of ice-sample density. In the density range 0.65 to 0.80 Mg m⁻³, the minimum strain rate decreases by an order of magnitude. At densities higher than 0.80 Mg m⁻³, however, the rate of minimum strain-rate decrease is lower, and the minimum strain rate at the close-off density is within a factor of two of that for dense (i.e. 0.912 Mg m⁻³) ice.

Mellor and Smith's (1966) figure 4 suggests that within the range 0.65 to 0.83 Mg m⁻³, the effect of density on strain rate is independent of temperature. The dashed line of Figure 1 has the same slope as the lines in the above density range from Mellor and Smith. Similarly, the dotted line of Figure 1 has the same slope as the line from Haefeli and von Sury's (1975) figure 7. While Mellor and Smith's samples were laboratory prepared, Haefeli and von Sury's were surface firn samples collected on the EGIG traverse of Greenland. The strain-rate dependence on density from these two studies agrees well with the present study. In addition, the present study extends the data to include densities between close-off and dense ice.

Figure 2 is a plot of total axial strain at minimum strain rate as a function of sample density. It is clear that

Table 1. Results of tests concerning the effect of density on minimum ice strain rate

Depth from ice core	Initial density	Density relative to dense ice	Minimum octahedral strain rate	Relative minimum strain rate	Strain at minimum strain rate	Final density
m	Mgm ⁻³		s ⁻¹		%	Mgm ⁻³
31	0.659	0.723	1.57 × 10 ⁻⁷	11.2	4.31	0.739
34	0.670	0.735	1.22 × 10 ⁻⁷	8.7	7.22	0.693
34	0.683	0.749	1.54 × 10 ⁻⁷	11.0	1.86	0.703
42	0.693	0.760	1.30 × 10 ⁻⁷	9.3	3.22	0.724
42	0.706	0.774	1.12 × 10 ⁻⁷	8.0	2.36	0.736
45	0.735	0.806	4.20 × 10 ⁻⁸	3.0	2.01	0.760
45	0.700	0.768	9.30 × 10 ⁻⁸	6.6	1.38	0.770
46	0.719	0.788	6.00 × 10 ⁻⁸	4.3	2.06	0.733
46	0.719	0.788	7.00 × 10 ⁻⁸	5.0	1.57	0.728
50	0.756	0.829	3.10 × 10 ⁻⁸	2.2	1.62	0.770
59.5	0.790	0.866	2.30 × 10 ⁻⁸	1.6	0.76	0.800
60	0.791	0.867	2.50 × 10 ⁻⁸	1.8	0.74	0.807
66	0.814	0.892	2.40 × 10 ⁻⁸	1.7	0.97	0.809
66	0.827	0.907	1.80 × 10 ⁻⁸	1.3	1.02	0.823
78	0.818	0.897	2.80 × 10 ⁻⁸	2.0	0.59	0.826
78	0.858	0.941	1.60 × 10 ⁻⁸	1.1	1.03	0.861
83	0.870	0.954	1.30 × 10 ⁻⁸	0.9	1.05	0.873
83	0.875	0.959	1.80 × 10 ⁻⁸	1.3	1.77	0.873
122	0.891	0.977	1.30 × 10 ⁻⁸	0.9	1.08	0.897
laboratory	0.912	1.000	1.10 × 10 ⁻⁸	0.8	0.71	0.912
laboratory	0.912	1.000	1.40 × 10 ⁻⁸	1.0	0.72	0.912
laboratory	0.912	1.000	2.00 × 10 ⁻⁸	1.4	0.93	0.912
laboratory	0.912	1.000	1.10 × 10 ⁻⁸	0.8	0.68	0.912

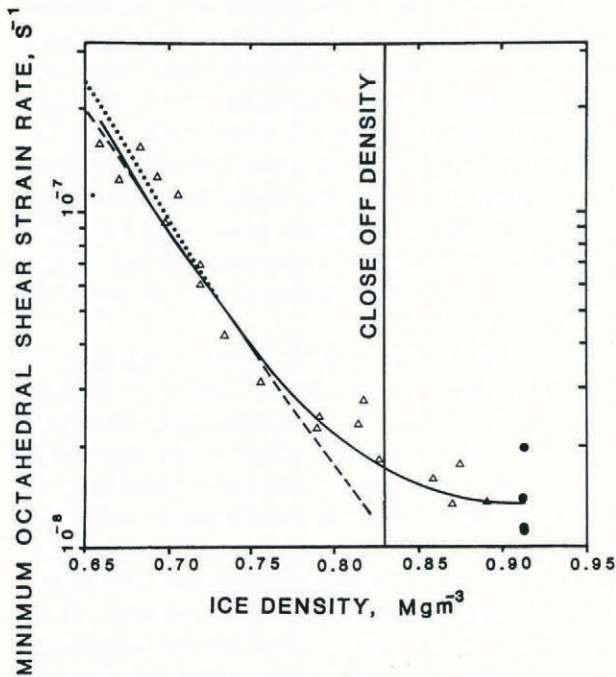


Fig. 1. Plot of minimum octahedral shear strain rate (measured in compression) as a function of ice-sample density, compared with the results obtained by Haefeli and von Sury (1975) (dotted line) and Mellor and Smith (1966) (dashed line). Data from laboratory sample tests are shown as dots; data from ice-core sample tests are shown as triangles.

this parameter too is affected little by sample density at values above the close-off density. The total strain value at minimum strain rate (~1%) for the high-density ice agrees well with the results for isotropic fine-grained ice of Mellor and Cole (1982) and Jacka (1984a).

The strain at minimum strain rate for the lower density ice is density-dependent, increasing to 6 to 8% for

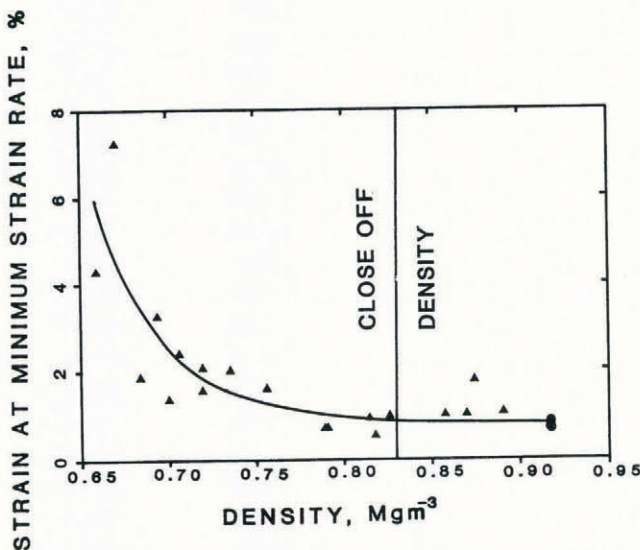


Fig. 2. Plot of total axial strain at minimum strain rate as a function of initial sample density.

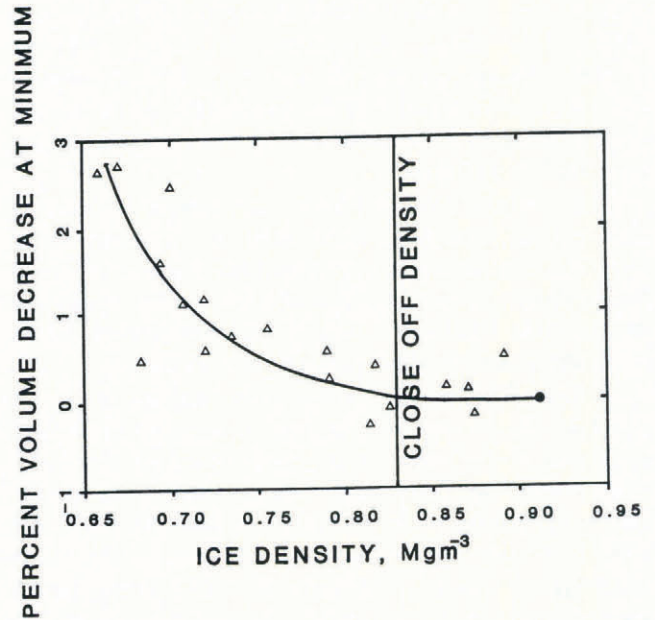


Fig. 3. Plot of per cent volume decrease at minimum strain rate as a function of initial sample density.

ice with density, 0.65 Mg m^{-3} . Some of this extra strain expended in attaining minimum strain rate is due to densification of the sample. The densification for the solid ice is zero and the lower the initial density, the higher the amount of densification possible. The amount of densification can be measured by the volume change in the sample. Figure 3 is a plot of per cent volume decrease at minimum strain rate as a function of initial density. The volume decrease was estimated by measuring the sample density before and after each experiment and by assuming conservation of mass. Experiments were terminated at different final strains, each one well beyond that at minimum strain rate. For the calculation of volume change up to minimum therefore, it has also been assumed that the densification process is linear with experiment duration. The densification process in natural ice sheets is certainly not linear (e.g. Bader, 1954), however the approximation over the very small density changes observed here will not be too unreasonable.

Comparison of Figures 2 and 3 shows that densification does not account for all of the additional strain (compared to high-density ice) required by the low-density material to attain minimum strain rate. The remainder of the strain needs therefore to be accounted for within a study of the mechanical properties of low-density ice (snow). This is beyond the scope of this paper, and the reader is referred to the reviews of this topic, e.g. Mellor (1975).

SAMPLE SHAPE AND SIZE

Uniaxial compression of cylindrical samples

Most laboratory studies of the uniaxial deformation of cylindrical ice samples have not determined the dependence of the test results on sample size or shape. Some experimenters have recommended that to minimise end

Table 2. Minimum strain-rate results for cylindrical samples of various shapes and sizes in uniaxial compression

Sample diameter	Sample length	Aspect ratio	Mean crystal diameter	Sample diameter/crystal diameter	Minimum octahedral shear strain rate
d(mm)	l(mm)	l/d	D(mm)	d/D	$\dot{\epsilon}_{\text{omin}} \text{ (s}^{-1}\text{)}$
64.9	68.1	1.05	1.4	46	1.45×10^{-8}
53.3	66.0	1.24	1.4	38	1.55×10^{-8}
40.8	62.0	1.52	1.4	29	1.70×10^{-8}
25.4	64.1	2.52	1.4	18	2.95×10^{-8}
17.0	70.0	4.112	1.4	12	3.40×10^{-8}
64.6	67.7	1.05	2.9	22	1.30×10^{-8}
52.5	66.3	1.26	2.9	18	1.50×10^{-8}
41.1	67.6	1.64	2.9	14	1.40×10^{-8}
24.8	60.4	2.44	2.9	8.6	3.30×10^{-8}
16.2	62.3	3.85	2.9	5.6	4.15×10^{-8}
53.2	65.8	1.24	1.4	38	1.70×10^{-8}
41.3	65.4	1.58	1.4	30	1.75×10^{-8}
33.8	65.2	1.93	1.4	24	2.55×10^{-8}
25.4	63.5	2.50	1.4	18	2.35×10^{-8}
16.3	61.5	3.77	1.4	12	2.70×10^{-8}
25.4	17.4	0.69	1.4	18	2.30×10^{-8}
25.4	28.7	1.13	1.4	18	2.70×10^{-8}
25.4	28.7	1.13	1.4	18	2.70×10^{-8}
25.4	96.5	3.80	1.4	18	1.95×10^{-8}
25.4	132.3	5.21	1.4	18	2.25×10^{-8}
25.4	22.1	0.87	1.4	18	2.55×10^{-8}
25.4	36.9	1.45	1.4	18	2.20×10^{-8}
25.4	50.1	1.97	1.4	18	2.15×10^{-8}
25.4	78.2	3.08	1.4	18	2.10×10^{-8}
25.4	115.8	4.56	1.4	18	2.30×10^{-8}
90.0	80.0	0.88	1.4	64	1.10×10^{-8}
90.0	65.0	0.72	1.4	64	1.05×10^{-8}
90.0	20.0	0.22	1.4	64	1.00×10^{-8}

effects during deformation in compression or extension, sample length, l to diameter, d ratios should be greater than 1. High values of l/d for compression may lead, particularly at high strains, to instabilities in the sample geometry, and an l/d value of approximately 3 has commonly been chosen (Mellor and Cole, 1983; Jones and Chew, 1983; Jacka, 1984a).

No systematic comprehensive study of the effect of sample shape or size on ice deformation exists. Theoretical and laboratory studies have been published, however, concerning size and shape effects on the deformation of other substances including ceramics (Birch and others, 1976), concrete (Symons, 1970) and rubber-like materials (Ogden, 1978). A review of uniaxial testing of rocks (Hawkes and Mellor, 1970) and subsequent application to ice testing (Hawkes and Mellor, 1972) summarises the problem at hand. Typically, uniaxial compression is applied through a platen or plunger such that a bond is created between the platen and the test material. This provides a radial constraint (usually complete) at both end planes and thus a non-

uniform stress field within the sample. This is well illustrated by visual examination of ice samples strained to high values (10% or more), which exhibit barrelling, the ends of the samples having diameters unchanged from the initial sample diameter. A uniform stress field compatible with the applied load will exist only if the sample is completely unrestrained radially and circumferentially along the entire sample length.

The platens used to hold the ice samples in position during the tests described in this paper are constructed of "Bakelite"—an incompressible resin-impregnated cloth material exhibiting high thermal insulation properties. This material has been used extensively in ice-deformation tests. For the compression tests, the platen is not (deliberately) fixed to the ice sample. The platen is fabricated in a cup shape and its purpose is only to act as a guide, i.e. to stop the sample from falling over during the loading stages of the test. However, it has been noticed that the ice affixes to the platen immediately the experimental load is applied. Thus, for the duration of the test, complete radial constraint does persist.

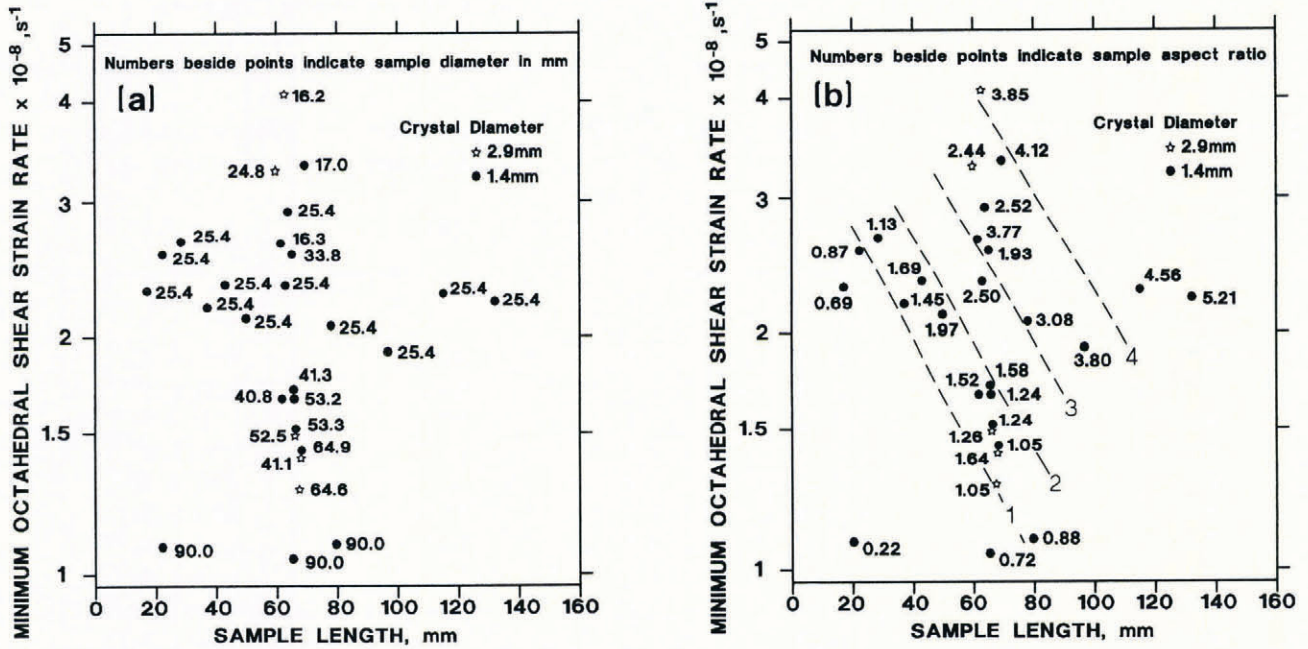


Fig. 4. Minimum octahedral shear strain rate plotted as a function of sample length for all data points. Two crystal sizes are indicated while numbers beside points are (a) sample diameter in mm, and (b) sample aspect ratio. Also shown in (b) are contours (dashed lines) of aspect ratio.

In order to achieve a uniform stress field, Hsu (1979) has recommended that PTFE (Teflon) sheet be placed between the platens and test material. For unconfined compression of cylindrical steel samples, Brownrigg and others (1981) have had some success with this technique. The PTFE does not act just as a lubricant. During the initial test stages, the PTFE is squeezed outwards until the outside rim of the sample encloses a bubble between the sample end and the platen. Hydrostatic pressure within

this PTFE bubble then exerts an outward radial force during further compression. The thickness of the PTFE sheeting is therefore critical. If it is too thick, the sample will assume a bollard shape. For steel test samples, a PTFE thickness to sample diameter ratio of 0.01 was found by Brownrigg and others (1981) to produce the same stress-strain behaviour over a range of sample diameters. Attempts to use PTFE in the manner described above for ice tests have so far been unsuccessful.

Thorough theoretical consideration of the internal distribution of stresses and displacements for circular cylinders of elastic materials was first given by Filon (1902). His solutions were later improved by Timoshenko (1934), Pickett (1944) (who gave a detailed explanation of the boundary conditions imposed by near-complete radial constraint at the platen/material interface) and by Balla (1960). In each of these papers, solutions for the stress distribution within a cylindrical specimen were obtained numerically and involved Fourier series with Bessel function coefficients. Each of the solutions exhibit a stress-field dependence on the cylinder aspect ratio (or slenderness), l/d , but not on the absolute dimensions (Balla, 1960). For the deformation of viscous material between two plates, Jaeger (1971) also found that the stress field was dependent upon the ratio of the distance between the platens and the platen radial dimension.

For the set of uniaxial compression tests described here, two moulds were used in the sample-making process, one of 25.4 mm internal diameter, and the other of 100 mm internal diameter. Test samples of various diameters were produced by turning down samples from one or the other mould. An octahedral shear stress of 0.25 MPa was applied to the samples and the test temperature was -5.0°C . Two separate grain-sizes were chosen (by sieving ice particles during the preparation of

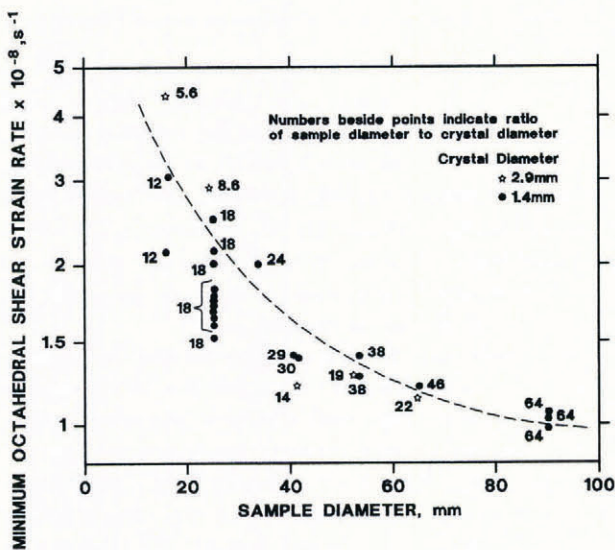


Fig. 5. Minimum octahedral shear strain rate as a function of sample diameter. Two crystal sizes are indicated and the numbers beside each point are sample diameter to crystal diameter ratio, d/D .

Table 3. Minimum strain-rate results for rectangular prism samples of various shapes and sizes in simple shear

Sample length	Sample height	Sample width	Length/height	Length/width	Height/width	Minimum strain rate
L	H	W	L/H	L/W	H/W	$\dot{\epsilon}_m$
mm	mm	mm				s ⁻¹
42.50	19.94	10.04	2.13	4.23	1.99	2.30×10^{-7}
63.60	15.98	9.42	3.98	6.75	1.70	2.00×10^{-7}
81.25	20.52	9.48	3.96	8.57	2.17	1.30×10^{-7}
98.70	21.55	10.10	4.58	9.77	2.13	2.50×10^{-7}
123.18	20.87	9.21	5.90	13.37	2.27	1.40×10^{-7}
136.76	20.30	7.44	6.74	18.38	2.73	1.10×10^{-7}
146.02	20.96	10.09	6.97	14.47	2.08	1.50×10^{-7}
146.77	20.50	8.50	7.16	17.27	2.41	1.10×10^{-7}
39.75	9.85	19.75	4.04	2.01	0.50	2.80×10^{-7}
37.94	16.50	20.92	2.30	1.81	0.79	1.30×10^{-7}
40.20	26.56	19.00	1.51	2.12	1.40	2.50×10^{-7}
40.69	32.67	21.10	1.25	1.93	1.55	1.80×10^{-7}
39.80	38.76	19.85	1.03	2.01	1.95	1.80×10^{-7}
42.40	45.40	20.42	0.94	2.08	2.22	1.80×10^{-7}
38.01	20.70	18.81	1.84	2.02	1.10	1.80×10^{-7}
41.08	20.54	23.80	2.00	1.73	0.86	1.30×10^{-7}
41.15	20.35	29.63	2.02	1.39	0.69	1.80×10^{-7}
40.99	20.74	33.87	1.98	1.12	0.61	1.60×10^{-7}
40.15	20.75	38.48	1.93	1.04	0.54	1.20×10^{-7}

the samples) so that the effect of crystal size, and of sample-size to crystal-size ratio, on deformation rates could be studied. Before testing, the sample mean crystal size was determined by counting the number of grains per unit area from enlarged thin-section photographs taken through crossed polaroids. Mean crystal diameter was estimated by assuming circular crystal cross-sections. Crystal orientation was determined from thin sections cut from the test samples prior to testing. Universal stage analysis consistently indicated approximately random crystal orientation fabrics.

Twenty-eight samples were tested for size effects. For 16 of these, the test sample length was set between 60 and 70 mm while diameters ranged from 16.2 mm to 90.0 mm. Twelve samples with diameters of 25.4 mm had lengths ranging from 174. to 132.3 mm and three samples of 90 mm diameter had lengths of 20.0, 65.0 and 80.0 mm. The total range of aspect ratio, l/d , covered by the experiments was 0.22 to 5.21. Two mean crystal sizes (1.4 and 2.9 mm diameter) were represented, and with some overlap of the above classes, the effect of sample length, l , sample diameter, d , aspect ratio, l/d , crystal diameter, D , and sample diameter to crystal diameter ratio, d/D were each able to be assessed independently.

Table 2 summarises results at minimum strain rate. Figure 4 shows plots of minimum octahedral shear strain rate, $\dot{\epsilon}_{0\min}$ as a function of sample length for each test. Sample diameter, d , is indicated in Figure 4a beside each data point. It is seen from the data points for samples of

25.4 mm diameter that sample length has little effect on the minimum strain rate. There is, however, a clear pattern of smaller minimum strain rates for larger sample diameters.

In Figure 4b sample aspect ratio, l/d , is indicated beside each point, and contours of constant aspect ratio are shown as dashed lines. It is seen that even for constant aspect ratio, strain rate decreases with increased sample diameter.

Figure 5 shows a plot of minimum strain rate, $\dot{\epsilon}_{0\min}$, as a function of sample diameter. The tendency to lower minimum strain rate for larger sample diameter is clear. There is some indication that for large enough sample diameter (larger than 100 mm) minimum strain rate may cease to be dependent on this parameter. Because of the high loads required to run tests on samples with diameters greater than 100 mm, these tests are difficult to conduct. At lower stresses (thus requiring smaller loads) tests take an unacceptably long time to attain minimum strain rate.

Simple shear of rectangular prism samples

Rectangular prism ice samples were prepared by first making cylindrical samples by the method of Jacka and Lile (1984), then cutting these to shape and to various sizes using a band saw. The range of sample lengths was 37.94 to 146.77 mm; of heights, 9.85 to 45.40 mm; and widths, 7.44 to 38.48 mm. To test the effect that these different sample dimensions might have on ice deform-

ation rate, 19 samples were deformed in simple shear at an octahedral shear stress of 0.2 MPa and temperature of -2.0°C . All tests were run beyond minimum strain rate. The shear apparatus and further details of these tests have been presented by Gao (1992).

Results are presented in Table 3. In shear there appears to be little dependence of minimum strain rate on sample dimensions or on sample dimension ratios. All minima are similar to within a factor of ~ 2.3 and there appears to be no evidence of any systematic trend in the minimum strain rates.

CRYSTAL DIAMETER AND RATIO OF CRYSTAL DIAMETER TO SAMPLE DIAMETER

In Figure 5, the numbers alongside each data point represent the ratio of sample diameter, d , to crystal diameter, D . There is no indication of this parameter affecting the minimum strain rate. Note in particular that samples of the same diameter but different crystal size exhibit similar minimum strain rates, while samples of different diameters but similar crystal size exhibit different minimum strain rates.

Jones and Chew (1981, 1983) concluded for their constant strain-rate tests at $5 \times 10^{-4} \text{ s}^{-1}$, that the

maximum yield stress was dependent on the ratio of sample diameter to crystal diameter, only for ratios less than ~ 12 . In order to vary this ratio, they varied the sample diameter, while the crystal diameter was unchanged at 1 mm. Results presented here suggest that it may have been the variation in sample diameter which resulted in different maximum yield stresses. Variations in crystal diameter within samples of the same diameter presented here did not affect the minimum flow rate, despite sample-diameter to crystal-diameter ratios as low as 6.

CONCLUSIONS

Density

Provided the density of ice is greater than at close off (i.e. $\sim 0.83 \text{ Mg m}^{-3}$) the minimum strain rate seems unaffected by this parameter. While this result is a useful one for field, laboratory and computing studies of ice masses, it is not difficult to produce ice of density higher than this value in the laboratory. Therefore the result would seem to imply that discrepancies between the results of different laboratories examining the flow of ice are not accounted for by this parameter.

Table 4. Summary of published data normalised to a common temperature and stress

Reference	Sample diameter	Octahedral stress	Temperature	Minimum octahedral strain rate	Normalised minimum octahedral strain rate
	D	τ_0	θ	$\dot{\epsilon}_{0\text{min}}$	$\dot{\epsilon}_N$
	mm	MPa	$^{\circ}\text{C}$	s^{-1}	s^{-1}
(a) Data normalised to $\tau_N = 0.25 \text{ MPa}$, $\theta_N = -5.0^{\circ}\text{C}$					
1	9.00	0.25	-5.0	1.00×10^{-8}	1.00×10^{-8}
1	25.4	0.25	-5.0	2.95×10^{-8}	2.95×10^{-8}
1	25.4	0.25	-5.0	1.95×10^{-8}	1.95×10^{-8}
2	50.8	0.377	-5.0	7.21×10^{-8}	2.10×10^{-8}
2	50.8	0.377	-5.0	7.28×10^{-8}	2.12×10^{-8}
3	80	0.236	-4.6	1.33×10^{-8}	1.58×10^{-8}
(b) Data normalised to $\tau_N = 0.25 \text{ MPa}$, $\theta_N = -10.0^{\circ}\text{C}$					
4	25.4	0.26	-10.0	9.3×10^{-9}	8.27×10^{-9}
4	25.4	0.26	-10.0	1.2×10^{-8}	1.07×10^{-8}
5	19.5	0.26	-9.1	9.19×10^{-9}	8.17×10^{-9}
5	19.5	0.26	-9.1	9.54×10^{-8}	8.48×10^{-8}
3	80	0.231	-7.2	2.89×10^{-9}	3.66×10^{-9}

References:

1. This study — one value at 90.0 mm diameter, at the highest and lowest minimum strain rate recorded for a diameter of 25.4 mm over the entire sample length range examined.
2. Mellor and Cole (1982) — two points at their lowest stress and therefore as close as possible to 0.25 MPa.
3. Duval and LeGac (1980) — one point at -4.6°C and the lowest (and therefore most likely to be at minimum) strain rate at -7.2°C .
4. Jacka (1984b) — the highest and lowest minimum strain rate recorded over the range of crystal sizes studied.
5. Baker (1978) — the highest and lowest secondary creep rate recorded over the range of crystal sizes studied.

Sample shape and size

In compression, evidence has been found that the sample diameter, but not sample length or aspect ratio, affects the minimum ice-creep rate. It also seems that the ratio of sample diameter to crystal diameter has little affect on the creep rate.

Examination of published results of uniaxial compression tests on polycrystalline ice, to ascertain whether the diameter effect found here accounts for inter-laboratory discrepancies, is hindered by several factors. Unfortunately the various ice mechanics experiments have not, in the past, chosen a common test temperature, stress, crystal size or sample size and shape. It is thus difficult to compare results directly. For direct comparison of published results, it is essential that these results have attained minimum strain rate, that the sample diameter is known and they they be considered at the same temperature and stress. Since very few published results are available which include all of these data, it has been necessary to consider experiments at stresses and temperatures near to the same value and to apply a normalising technique.

The equation (Hooke and others, 1972)

$$\dot{\epsilon}_N = \dot{\epsilon}_{0min} (\tau_N/\tau_o)^n \exp\left(\frac{Q}{R}\left(\frac{1}{\theta} - \frac{1}{\theta_N}\right)\right) \quad (1)$$

was used to convert published minimum octahedral shear strain rates, $\dot{\epsilon}_{o min}$ at octahedral shear stress, τ_o and temperature, $\theta(K)$ to normalised minimum octahedral shear strain rates, $\dot{\epsilon}_N$ pertaining to an octahedral shear stress, τ_N and temperature, $\theta_N(K)$. $R = 8.314 J mol^{-1} K^{-1}$ is the gas constant, and Q is the ice-creep activation energy. $Q \approx 162 kJ mol^{-1}$ at $-5^\circ C$ and $100 kJ mol^{-1}$ at $-10^\circ C$. For the current exercise, the ice-creep power law exponent, n was taken as 3.

Table 4 displays a summary of data used for a comparison of results of published data. The data have all been adjusted to the same units and to octahedral values. The righthand column of Table 4a shows the minimum octahedral shear-strain rates normalised to $-5^\circ C$ at 0.25 MPa (which includes data recorded at temperatures and stresses near to these values). Table 4b comes from three papers which deal with the effect of crystal size on ice-creep rates. Those studies were done at temperatures near $-10^\circ C$.

Figure 6 shows plots of normalised data. The dashed curve on the plots comes from Figure 5. Secondary creep rates observed by Baker (1978) are considerably higher than those observed by Jacka (1984b) at approximately the same temperature and stress. Secondary creep rates found by Duval and LeGac (1980) are lower. Duval and LeGac in fact normalised their own and Baker's results to a common temperature and stress, and noted that their minimum strain rates were for every test, substantially lower than Baker's. Baker's sample diameters were 19 mm. Jacka's samples diameters were 25.4 mm diameter. The Duval and LeGac sample diameters were 80 mm. These data provide some evidence to demonstrate that the effect of sample diameter on creep-rate results may account for some of the discrepancies which have been noted between various studies.

A final dilemma arising from the above findings concerns the relation between results from laboratory experiments and the flow of natural ice masses. While further theoretical and experimental study continues on the stress distribution within laboratory deforming ice

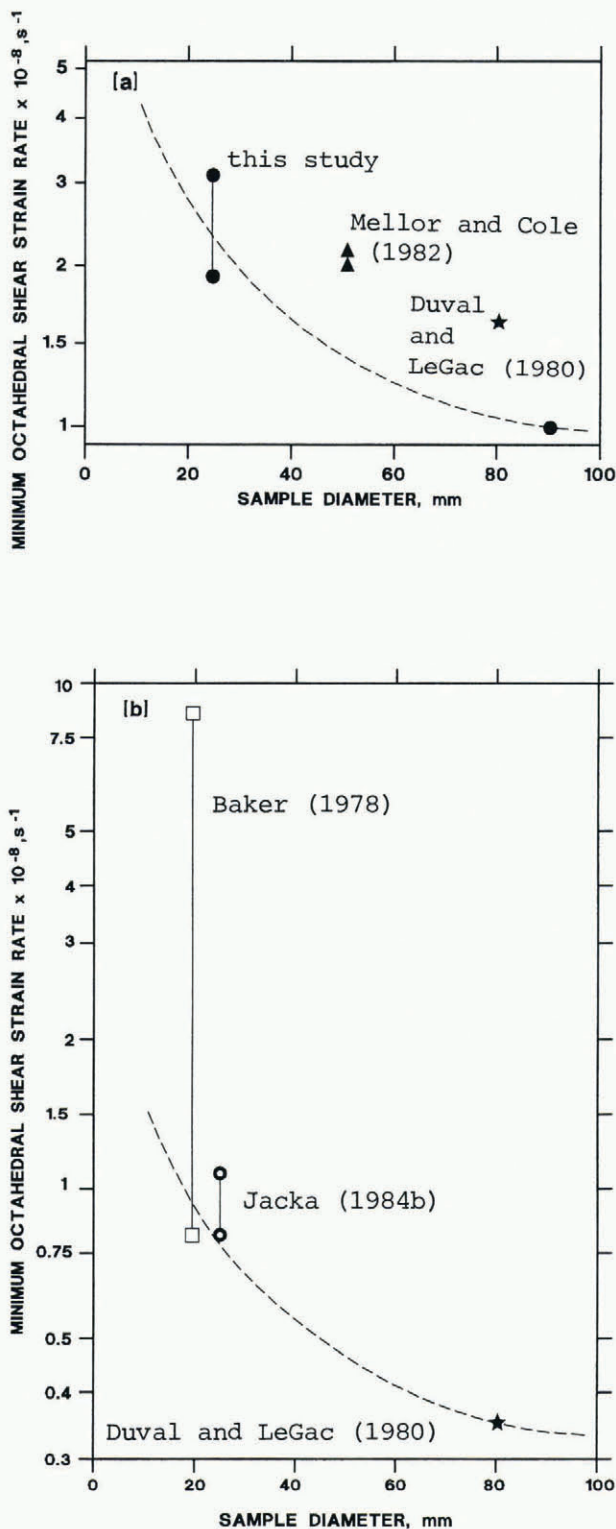


Fig. 6. Minimum octahedral shear strain rates from past published studies, plotted as a function of sample diameter for results normalised to a, $\tau_N = 0.25 MPa, \theta_N = -5.0^\circ C$ and b, $\tau_N = 0.25 MPa, \theta_N = -10.0^\circ C$. The curves are parallel to the curve of Figure 5.

samples, for the time being the most convenient solution to this problem may be by direct comparison of field measurements with laboratory measurements.

Above all, the findings highlight the need for experimenters to publish data resulting from their work in detail. Inter-laboratory comparison of data are made especially difficult if the usefulness of good quality results is lessened by failure to include basic yet essential information such as preparation technique, experimental technique, sample dimensions, etc.

ACKNOWLEDGEMENTS

I thank Scott Williams, Gao Xiang Qun and Li Jun for carrying out several of the experiments utilised in this paper.

REFERENCES

- Bader, H. 1954. Sorge's law of densification of snow on high polar glaciers. *J. Glaciol.*, **2**(15), 319–323.
- Baker, R. W. 1978. The influence of ice-crystal size on creep. *J. Glaciol.*, **21**(85), 485–500.
- Balla, A. 1960. Stress conditions in tri-axial compression. *Am. Soc. Civ. Eng. Soil Mech. Found. Div.*, **86**(SM6), 57–84.
- Birch, J. M., B. Wilshire, D. J. R. Owen and D. Shantaram. 1976. The influence of stress distribution on the deformation and fracture behaviour of ceramic materials under compression creep conditions. *J. Mater. Sci.*, **11**, 1817–1825.
- Brownrigg, A., J. Havranek and M. Littlejohn. 1981. Cold forgeability of steel. *BHP Technical Bulletin*, **25**(2), 16–23.
- Duval, P. and H. Le Gac. 1980. Does the permanent creep-rate of polycrystalline ice increase with crystal size? *J. Glaciol.*, **25**(91), 151–157.
- Filon, L. N. G. 1902. On the elastic equilibrium of circular cylinders under certain practical systems of load. *Philos. Trans. R. Soc. London, Ser. A*, **198**, 147–233.
- Gao, X. Q. 1992. Laboratory studies of the development of anisotropic crystal structure and the flow properties of ice. (Ph.D. thesis, University of Melbourne.)
- Haefeli, R. and H. von Sury. 1975. Strain and stress in snow, firn and ice along the EGIG profile of the Greenland ice sheet. *International Association of Hydrological Sciences Publication 114* (Symposium at Grindelwald 1974—*Snow Mechanics*), 342–352.
- Hawkes, I. and M. Mellor. 1970. Uniaxial testing in rock mechanics laboratories. *Eng. Geol.*, **4**, 179–285.
- Hawkes, I. and M. Mellor. 1972. Deformation and fracture of ice under uniaxial stress. *J. Glaciol.*, **11**(61), 103–131.
- Hooke, R. LeB. 1981. Flow law for polycrystalline ice in glaciers: comparison of theoretical predictions, laboratory data, and field measurements. *Rev. Geophys. Space Phys.*, **19**(4), 664–672.
- Hooke, R. LeB., B. B. Dahlin and M. T. Kauper. 1972. Creep of ice containing dispersed fine sand. *J. Glaciol.*, **11**(63), 327–336.
- Hsu, T. C. 1979. A study of the compression test for ductile materials. *Mater. Res. Stand.*, **9**(12), 20.
- Jacka, T. H. 1984a. Laboratory studies on relationships between ice crystal size and flow rate. *Cold Reg. Sci. Technol.*, **10**(1), 31–42.
- Jacka, T. H. 1984b. The time and strain required for development of minimum strain rates in ice. *Cold Reg. Sci. Technol.*, **8**(3), 261–268.
- Jacka, T. H. and R. C. Lile. 1984. Sample preparation techniques and compression apparatus for ice flow studies. *Cold Reg. Sci. Technol.*, **8**(3), 235–240.
- Jaeger, J. C. 1971. *Elasticity, fracture and flow with engineering and geological applications*. London, Methuen.
- Jones, S. J. and H. A. M. Chew. 1981. On the grain-size dependence of secondary creep. *J. Glaciol.*, **27**(97), 517–518.
- Jones, S. J. and H. A. M. Chew. 1983. Effect of sample and grain size on the compressive strength of ice. *Ann. Glaciol.*, **4**, 129–132.
- Mellor, M. 1975. A review of basic snow mechanics. *International Association of Hydrological Sciences Publication 114* (Symposium at Grindelwald 1974—*Snow Mechanics*), 251–291.
- Mellor, M. and D. M. Cole. 1982. Deformation and failure of ice under constant stress or constant strain-rate. *Cold. Reg. Sci. Technol.*, **5**(3), 201–219.
- Mellor, M. and J. H. Smith. 1966. Creep of snow and ice. *CRREL Res. Rep.* 220.
- Morgan, V. I. 1979. A system for accurate temperature control of small fluid baths. *J. Glaciol.*, **22**(87), 389–391.
- Morgan, V. I., E. R. Davis and E. Wehrle. 1984. A Rigsby stage with remote computer compatible output. *Cold Reg. Sci. Technol.*, **10**(1), 89–92.
- Ogden, R. W. 1978. Nearly isochoric elastic deformations: application to rubberlike solids. *J. Mech. Phys. Solids*, **26**, 37–57.
- Paterson, W. S. B. 1981. *The physics of glaciers. Second edition*. Oxford, etc., Pergamon Press.
- Pickett, G. 1944. Application of the Fourier method to the solution of certain boundary problems in the theory of elasticity. *J. Appl. Mech.*, **2**, A176–A182.
- Symons, I. F. 1970. The effect of size and shape of specimen upon the unconfined compressive strength of cement-stabilised materials. *Mag. Concr. Res.*, **22**(70), 45–50.
- Timoshenko, S. 1934. *Theory of elasticity*. New York, McGraw-Hill Book Co.

The accuracy of references in the text and in this list is the responsibility of the author, to whom queries should be addressed.